Hydrogen Spillover on CeO_2/Pt: Enhanced Storage of Active Hydrogen

Gargi Dutta,[†] Umesh V. Waghmare,[†] Tinku Baidya,[‡] and M. S. Hegde*,[‡]

Theoretical Sciences Unit, Jawaharlal Nehru Centre for Advanced Scientific Research, Jakkur Campus, Bangalore 560 064, India, and Solid State and Structural Chemistry Unit, Indian Institute of Science, Bangalore 560 012, India

Received May 17, 2007. Revised Manuscript Received September 24, 2007

We have investigated the concept of hydrogen spillover by a density functional theory (DFT) approach in combination with experimental observations. A H/Pt molar ratio of 5 to 9 is observed over $Ce_{1-x}Pt_xO_{2-\delta}$ catalyst, where Pt is present in the +2 ionic state. The total hydrogen adsorbed over the catalyst is ~30 times higher than that over nano-Pt metal particles. NMR study show protonic hydrogen over the catalyst. DFT calculations indeed support the enhanced adsorption of hydrogen on the Pt-ion-doped ceria surface via spillover to the oxide support. Further, the calculations confirm the formation of protonic hydrogen on the catalyst surface in contrast to the formation of hydridic hydrogen on Pt metal.

1. Introduction

Hydrogen spillover is a concept developed in heterogeneous catalysis. This arose because the total number of hydrogen atoms adsorbed per Pt atom on Pt/Al_2O_3 catalyst was found to be more than one, whereas only one hydrogen atom is expected to be adsorbed per Pt atom.[1,2] Pt metal particles dispersed over carbon, alumina, and silica showed H/Pt surface ratio more than one and it was proposed that the extra hydrogen atoms spilled over to the support. The spillover phenomena are also observed for other molecules such as O_2. There exists extensive literature on spillover phenomena and it has been reviewed by Conner et al.[3,4]

Hydrogen adsorbed on Pt/Al_2O_3 can be reacted with oxygen to give H_2O, as O_2 is known to dissociate and chemisorb on the Pt surface.[5] Although dissociation of H_2 would facilitate H_2O formation, presence of dissociated hydrogen is not a necessary criterion. If the hydrogen molecule is chemisorbed and H−H bond in H_2 is weaker, it forms a precursor to dissociation, and dissociated oxygen can induce O−H bond formation by breaking a H−H bond.

In the H_2 spillover observed on Pt/Al_2O_3, the H/Pt ratio is about 2.5 at 200 °C. On the contrary, if Pt is dispersed over a reducible oxide support such as CeO_2 in the form of $Ce_{0.99}Pt_{0.01}O_{2-\delta}$, where Pt is in the +2 state even at room temperature, the H/Pt ratio is as high as 5.[6] Further, the rate of H_2 and O_2 recombination reactions is more than 50 times higher with $Ce_{0.99}Pt_{0.01}O_{2-\delta}$ compared to Pt metal nanoparticles.[7,8] Therefore, adsorption of H_2 on Pt^0 and Pt^{2+} ions in CeO_2 is expected to involve different mechanisms. Generally, Pt/C is used as both anode and cathode for (H_2 + O_2) fuel cell. Hydrogen dissociation and proton transport are very important for (H_2 + O_2) fuel cell applications and hence understanding of H_2 spillover on Pt^0 and Pt^2 ions in CeO_2 is crucial. There are a number of questions associated with hydrogen spillover: (a) Is the H_2 molecule on the Pt surface dissociated or it is just a precursor molecule to dissociation ? (b) Is the spilled over hydrogen in dissociated form? (c) If the spilled over hydrogen is a molecule, how is it accommodated on Al_2O_3 or CeO_2 oxide support surface? (d) Does Ce^{4+} or Al^{3+} ion act as active sites (Lewis acid) for spilled over hydrogen? (e) What is the charge ($+ve$ or $-ve$) of hydrogen adsorbed on Pt^0 or on Pt^{2+} in CeO_2? (f) What is the maximum distance from the Pt site within which hydrogen molecule/atom spills over to the oxide support surface? (g) Is there any short contact (hydrogen bond) with oxide ion such as $H\cdots H\cdots O^{2-}$ in Pt/CeO_2? As of now, there is no work relevant to these important issues, and H_2 spillover has been viewed in the catalysis literature as hydrogen adsorption phenomena with an excess H/Pt ratio higher than 1.

Our work is focused on the adsorption and catalytic activity of $Ce_{1-x}Pt_xO_{2-\delta}$ where Pt^{2+} ions are dispersed over CeO_2 crystallite surface; Pt^{2+} ion is substituted for Ce^{4+} ion with an oxide ion vacancy for charge compensation.[9] A high H_2/Pt ratio of 2.5 and high H_2 + O_2 recombination rate over this material compared to Pt^0 in Pt metal particles, as in Pt/Al_2O_3, motivated us to revisit the hydrogen spillover problem. We employed a systematic density functional theory (DFT) approach to determine configurations of adsorption of hydrogen on Pt and Pt/CeO_2 with the aim of answering most

* Corresponding author. E-mail: waghmare@jncasr.ac.in (U.M.W.); mshegde@sscu.iisc.ernet.in (M.S.H.).
† Jawaharlal Nehru Centre for Advanced Scientific Research.
‡ Indian Institute of Science.

(1) Ozaki, A. *Isotropic Studies of Heterogeneous Catalysis*; Academic Press: New York, 1977.
(2) Kuriacose, J. *Indian J. Chem.* **1957**, *5*, 646.
(3) Conner, W. C., Jr.; Falconer, J. L. *Chem. Rev.* **1995**, *95*, 759.
(4) Conner, W. C., Jr.; Pajonk, G. M.; Teichner, S. J. *Advances in Cataysis*; Academic Press: New York, 1986; Vol *34*, p 1.
(5) Roberts, M. W.; Mckee, C. S. *Chemistry of the Metal−Gas Interface*; Oxford University Press: Oxford, U.K., 1978; Chapter 11, p 439.
(6) Bera, P.; Gayen, A.; Hegde, M. S.; Lalla, N. P.; Spadaro, L.; Frusteri, F.; Arena, F. *J. Phys. Chem. B* **2003**, *107*, 6122.
(7) Hariprakash, B.; Bera, P.; Martha, S. K.; Gaffoor, S. A.; Hegde, M. S.; Shukla, A. K. *Electrochem. Solid-State Lett.* **2001**, *4*, A23.
(8) Bera, P.; Hegde, M. S.; Patil, K. C. *Curr. Sci.* **2001**, *80*, 1576.
(9) Bera, P.; Priolkar, K. R.; Gayen, A.; Sarode, P. R.; Hegde, M. S.; Emura, S.; Kumashiro, R.; Jayaram, V.; Subanna, G. N. *Chem. Mater.* **2003**, *15*, 2049.

10.1021/cm071330m CCC: $37.00
Published on Web 11/20/2007

of the questions on hydrogen spillover, and we corroborate our understanding with experimental verifications.

2. Experimental Methods

2.1. Experiment. Pure CeO_2 was prepared by solution combustion method, taking ammonium ceric nitrate ($(NH_4)_2Ce(NO_3)_6$ and oxalyl dihydrazide (ODH) ($C_2H_6N_4O_2$) in a 1:0.409 weight ratio. For routine preparation, 5 g of $(NH_4)_2Ce(NO_3)_6$ and 2.045 g of $C_2H_6N_4O_2$ were taken in a 300 mL crystallizing dish and made into a clear aqueous solution and then kept in the furnace at 400 °C, giving the product within a few minutes. $Ce_{1-x}Pt_xO_{2-\delta}$?(x = 0.005, 0.01, 0.02) solid solutions were also prepared by the solution combustion method. $Ce_{0.995}Pt_{0.005}O_{2-\delta}$ was prepared by making 10 g of ammonium ceric nitrate, 0.0385 g of H_2PtCl_6, and 5.8 g of ODH with 20 mL H_2O into clear solution in a 300 mL crystallizing dish and heating the solution in a muffle furnace at 400 °C. The solution boils and after complete dehydration ignites into flame, raising the temperature to ~1000 °C, dwelling ther for 30− 40 s, and then cooling to 400 °C. The product compounds were obtained within a few minutes. Similarly, 1 and 2 at % Pt-substituted CeO_2 were prepared. Nanosized Pt metal particles of 8 nm were prepared by polyol method. $Ce_{1-x}Pt_xO_{2-\delta}$ crystallizes in a fluorite structure with oxide ion vacancy around the Pt^{2+} ion; the structural details have been studied by P. Bera et al.[9]

Hydrogen adsorption/uptake was measured in a temperature-programmed reduction (H_2 -TPR) by passing a 5% H_2 + 95% Ar mixture at a 30 mL/min flow rate over 100 mg of oxide at a ramp rate of 10 °C/min. The H_2 uptake is detected by a thermal conductivity detector (TCD) and calibrated against the uptake of H_2 for a known amount of CuO.

A pulse H_2 adsorption experiment was carried out in the same instrument. Initially, H_2 was passed over the catalyst and H_2 uptake measured as a function of time at 32 °C. Oxygen was then passed over the catalyst at room temperature. Adsorbed H_2 did react with O_2, increasing the catalyst temperature to about 38 °C. Repeated H_2 uptake is carried out after reacting with O_2 each time.

NMR data were recorded in a DRX 500 MHz Bruker instrument. To carry out the H NMR experiment, we heated a Pt-substituted sample at 450 °C overnight to remove moisture. An NMR tube filled with sample grain was heated in ultrahigh pure (UHP) O_2 and then evacuated to 1×10^{-3} Torr. Pure H_2 was filled at atmospheric pressure and at room temperature. Core level photoelectron spectra (XPS) of the Pt ion in the Pt-ion-doped ceria is carried out in an ESCA-3 Mark II spectrometer of VG Scientific Ltd. equipped with a preparation chamber.

2.2. Theory. Our total energy calculations are based on the ABINIT[10,11] implementation of DFT[12] and exchange-correlation energy within the local density approximation (LDA[13]). It involves solving the Kohn–Sham equations[14] by a fixed-potential-based iterative conjugate-gradient minimization[15] of one-electron energies in the ground-state and achieves the self-consistency of the Kohn–Sham potential.[16] The potential of the nucleus and the core electrons was approximated with pseudopotentials: Fritz-Haber-Institute pseudopotentials were used for Ce, O, and Pt and

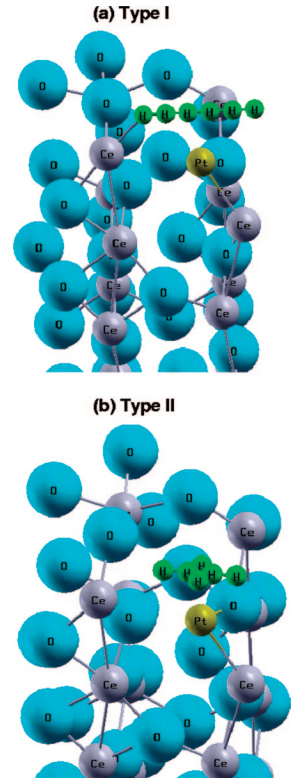

Figure 1. Type I and II initial configurations of the 6-H CeO_2 /Pt system. In this case, type II is found to be more stable.

Troullier−Martins pseudopotentials for H. We used an energy cutoff of 25 Ha, a $2 \times 2 \times 2$ Monkhorst−Pack mesh[17] for Brillouin zone integration. Ionic relaxations were performed using a Broyden, Fletcher, Goldfarb, Shanno (BFGS)-based minimization[18] and molecular dynamics with viscous damping. We have performed Hirshfeld atomic charge analysis to understand the net charge on atoms and charge transfers between atoms.[19]

Our simulations of the CeO_2 (100) surface employ supercells of 16 formula units. In $Ce_{15}PtO_{31}$, one Ce has been substituted for Pt and one oxygen vacancy has been created to maintain the charge balance and Pt^{2+} state in the supercell. Configurations with hydrogen adsorbed on the Pt-doped CeO_2 surface consist of up to 7 hydrogens atoms. For each of the configurations with 4−7 H atoms, we have tried two configurations: (a) hydrogens arranged in a chain centered at Pt (type I) and (b) hydrogrens arranged in two mutually perpendicular lines centered at Pt (type II) (see Figure 1). In this paper, we report the most stable configurations for different numbers of hydrogen atoms. For 5 and 7 H's, type I, and for 4 and 6 H's, type II were found to be most stable. The initial configurations (type I) of 5 and 7 H/$Ce_{15}PtO_{31}$ have H's placed in the form of chain centered at Pt with a H−H distance of about 0.74 Å. For the 4-H case initial configuration (type II), two H's are placed with their bond centered at the Pt site and a H−H distance of 0.74 Å and the other two H's are placed similarly in a line perpendicular to the previous two H's on either side of the Pt site and an H−H distance of 0.74 Å. The type II configuration of 6 H is similar to that of the 4-H case. The 3-H case is type I, with one H on top of Pt site and the other two H's on either side with a H−H distance of 0.74 Å. For the 2-H case initial configuration, we have placed a hydrogen molecule (with a H−H distance of 0.74 Å) with the bond centered at Pt and for the 1-H case, we had a

(10) Gonze, X.; Beuken, J.-M.; Caracas, R.; Detraux, F.; Fuchs, M.; Rignanese, G.-M.; Sindic, L.; Verstraete, M.; Zerah, G.; Jollet, F.; Torrent, M.; Roy, A.; Mikami, M.; Ghosez, Ph.; Raty, J.-Y.; Allan, D. C. *Comput. Mater. Sci.* **2002**, *25*, 478; http://www.abinit.org.
(11) Goedecker, S. *SIAM J. Sci. Comput.* **1997**, *18*, 1605.
(12) Hohenberg, P.; Kohn, W. *Phys. Rev.* **1964**, *136*, 864B.
(13) Goedecker, S.; Teter, M.; Huetter, J. *Phys. Rev. B* **1996**, *54*, 1703.
(14) Kohn, W.; Sham, L. J. *Phys. Rev.* **1965**, *140*, 1133A.
(15) Payne, M. C.; Teter, M. P.; Allan, D. C.; Arias, T. A.; Joannopoulos, J. D. *Rev. Mod. Phys.* **1992**, *64*, 1045.
(16) Gonze, X. *Phys. Rev. B* **1996**, *54*, 4383.
(17) Monkhorst, H. J.; Pack, J. D. *Phys. Rev. B* **1976**, *13*, 5188.
(18) http://www.library.cornell.edu/nr/bookcpdf/c10–7.pdf.
(19) Hirshfeld, F. L. *Theor. Chim. Acta* **1977**, *44*, 129.

single hydrogen atom on top of Pt. Different initial configuration for different number of H's were chosen in order to ensure that our results are independent of the configuration of hydrogens and are dependent only on the number of hydrogens, i.e., on the concentration of hydrogen on the surface of the catalyst.

We have chosen a symmetrical slab of CeO_2 and both surfaces of the slab are oxygen-terminated (to cancel the intrinsic dipole moment which would have arose because of different termination, O on one surface and Ce on the other) with 50% O vacancy on one surface and removed the oxygens to the other surface in order to maintain the correct formula units. So both the surfaces have 50% oxygen vacancy and the occupied oxygen sites are same on both surfaces. Skorodumova et al.[20] discuss various models of oxygen termination for the CeO_2 (100) surface. On Pt doping in a slab of ceria, we have created another oxygen vacancy in the layer just below that of Pt as we have substituted a Ce^{4+} ion with a Pt^{2+} ion. Because of the partial O vacancy on the surfaces, Pt is exposed to the surface even though it is in the second layer of atoms in the slab. In the initial configurations, hydrogens were placed in a layer at a distance of ~1.8 Å from the Pt atom. The *c*/*a* ratio of the supercell is 3.64 in all the slab calculations with hydrogen ($a = b = 7.65$ Å, $c = 27.83$ Å). We have cerium and oxygen layers stacked in the *z*-direction and have used sufficient vacuum thickness of about 15−17 Å in our calculations to keep the slab−slab interaction negligible. Of the nine layers of alternately stacked O's and Ce's in the z-direction, the first layer contains 4 O's with 50% O-vacancy, the second layer contains 1 Pt and 3 Ce's, the third layer contains 7 O's (one O vacancy due to Pt doping), and then alternate layers contain 4 Ce's and 8 O's, and the ninth layer is again a surface layer with 4 O's and with 50% O vacancy. Hence, the formula for the slab without H's is $Ce_{15}PtO_{31}$, with a total of 47 atoms. In this work, we are interested only in the surface layer of atoms, as they are more important for catalytic activity than the bulk layers.

We had earlier calculated binding energies of bulk CeO_2, $CeO_{1.75}$, and structures of Zr/Ti-doped CeO_2 with oxygen vacancies.[21,22] The cost of creating an oxygen vacancy in bulk ceria is about 11.83 eV, and the cost of substituting Pt in the presence of an oxygen vacancy in a slab of ceria is about 10.61 eV. Hence, it is seen that substituting Pt for Ce is energetically favorable in the presence of oxygen vacancy by about 1.22 eV. Our earlier experiments have shown an oxide-ion vacancy in Pt-ion-doped ceria from a detailed analysis of EXAFS.[9]

3. Results

3.1. Experimental Observations. Figure 2 shows the H_2-TPR profile of $Ce_{0.995}Pt_{0.005}O_{2-\delta}$, $Ce_{0.99}Pt_{0.01}O_{2-\delta}$, and $Ce_{0.98}Pt_{0.02}O_{2-\delta}$ from −50 to 800 °C. Pure ceria does not adsorb hydrogen at low temperature; uptake due to the removal of surface oxygen is observed at 470 °C, and the reduction of surface oxygen corresponds to the composition of $CeO_{1.91}$. With the Pt ion substitution, the H_2 uptake temperature decreases to 390 °C in addition to peaks at low temperature. The peak at 165 °C is possibly associated with the removal of oxygen bonded to Pt ion and Ce ion. The intensity of this peak also decreases and major peaks with enhanced intensity are observed at 5 °C on 1 and 2 at % Pt in ceria. Note

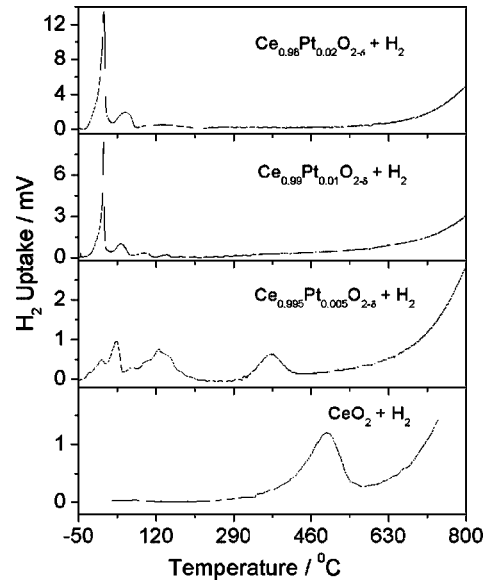

Figure 2. H_2 TPR profile of $Ce_{0.995}Pt_{0.005}O_{2n-\delta}$, $Ce_{0.99}Pt_{0.01}O_{2-\delta}$, and $Ce_{0.98}Pt_{0.02}O_{2-\delta}$.

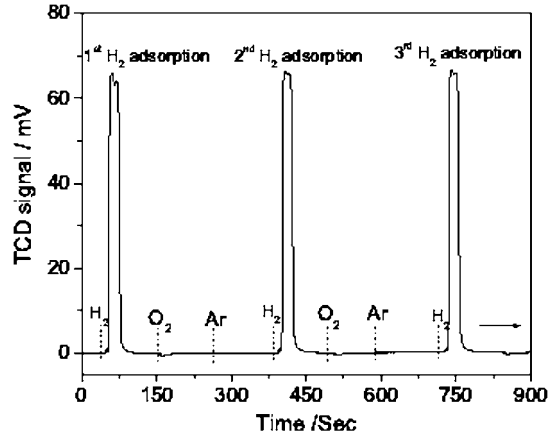

Figure 3. Pulse H_2 adsorption experiment for three cycles.

Y-scales are different for different samples. Molar H/Pt ratios were 8.6, 4.8, and 2.8 over $Ce_{0.995}Pt_{0.005}O_{2-\delta}$, $Ce_{0.99}Pt_{0.01}O_{2-\delta}$, and $Ce_{0.98}Pt_{0.02}O_{2-\delta}$, respectively. Pt is present in the +2 state in the compound and if Pt^{2+} ion is reduced to Pt^0 with the reaction $Pt^{2+} + H_2 \rightarrow Pt^0 + 2H^+$, the H/Pt ratio should have been ~2. Clearly, the H/Pt ratio is much higher than 2. The hydrogen uptake experiment from our earlier work was carried out with $H_2Pt(OH)_6$, where Pt is in the +4 state. The peak reduction temperature observed is 40 °C, and total hydrogen taken up corresponded to the reaction $Pt^{4+} + 2H_2 \rightarrow Pt^0 + 4H^+$.[6] We do not observe hydroxyl ion formation. To test the strength of H_2 adsorption, we carried out a pulse experiment over $Ce_{0.99}Pt_{0.01}O_{2-\delta}$ at room temperature (32 °C). Figure 3 shows the three cycles of H_2 adsorption on the catalyst followed by oxygen adsorption after each cycle. When O_2 was passed after H_2 adsorption, there was an increase in temperature from 32 to 38 °C that is due to the exothermic nature of the reaction $H_2 + O_2 \rightarrow H_2O$. The formation of H_2O was observed with a quadrapole mass spectrometer. The H/Pt ratio in the pulse experiment was ~5 for $Ce_{0.99}Pt_{0.01}O_{2-\delta}$ each time. With only nano Pt metal particles, prepared by the polyol method, the H_2 adsorption

(20) Skorodumova, N. V.; Baudin, M.; Hermansson, K. *Phys. Rev. B.* **2004**, *69*, 075401.
(21) Dutta, G.; Waghmare, U. V.; Baidya, T.; Hegde, M. S.; Priolkar, K. R.; Sarode, P. R. *Catal. Lett.* **2006**, *108*, 165.
(22) Dutta, G.; Waghmare, U. V.; Baidya, T.; Hegde, M. S.; Priolkar, K. R.; Sarode, P. R. *Chem. Mater.* **2006**, *18*, 3249.

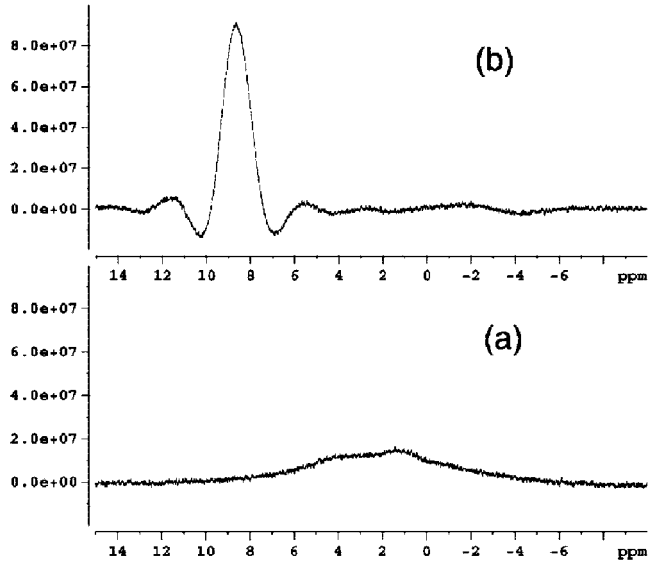

Figure 4. H NMR (a) without and (b) with hydrogen adsorbed on $Ce_{0.99}Pt_{0.01}O_{2-\delta}$.

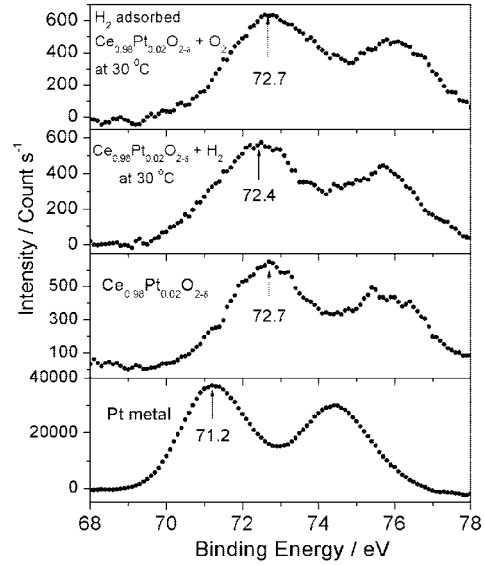

Figure 5. XPS of Pt(4f) core level in Pt metal, $Ce_{0.98}Pt_{0.02}O_{2-\delta}$, $Ce_{0.98}Pt_{0.02}O_{2-\delta} + H_2$ at 30 °C, H_2 adsorbed $Ce_{0.98}Pt_{0.02}O_{2-\delta} + O_2$ at 30 °C.

experiment showed the H/Pt ratio of 0.164 and thus more than 30 times more hydrogen adsorbed when Pt^{2+} ions are dispersed in CeO_2 compared to Pt^0 in Pt nanoparticles for same amount of Pt at room temperature. If we take into account only the surface Pt atoms in the metal particles for H_2 adsorption, the total H/Pt ratio of 0.164 translates into $H/Pt_{surface} \approx 0.9$, again indicating one hydrogen atom per surface Pt atom.

To find the interaction of H_2 with the catalysts, we carried out an NMR study. Figure 4 shows the H NMR of H_2 adsorbed surface as well as the as-prepared sample for comparison. A small peak observed over $Ce_{0.99}Pt_{0.01}O_{2-\delta}$ without adsorbed hydrogen may be due to adsorbed H_2O. A single peak at ~8 ppm is observed in the H_2-adsorbed sample. The high field shift falls in the proton region. Thus, adsorbed hydrogen in the catalyst is protonic ($H^{\delta+}$ or $H_2{}^{\delta+}$).

Core level binding energy shift of a metal ion with respect to metal is directly proportional to the effective charge on the ion.[23] We have completed an XPS study of Pt-ion-substituted ceria with and without hydrogen. Hydrogen was adsorbed in situ. In Figure 5, we have shown the Pt(4f) core level spectra in Pt metal, $Ce_{0.98}Pt_{0.02}O_{2-\delta}$, after saturated hydrogen adsorption at room temperature in the spectrometer and after oxygen exposure to the hydrogen-adsorbed sample. ThePt(4f 7/2) peak is shifted from 71.2 eV in the Pt metal to 72.7 eV in the Pt-doped ceria; the shift corresponds to Pt in the +2 formal oxidation state. Upon hydrogen adsorption, the peak is shifted to lower binding energy by about 0.3 eV. The surface is now exposed to oxygen to react with adsorbed hydrogen. The Pt(4f) peak is shifted back to 72.7 eV. On saturated hydrogen coverage, ionic Pt is not fully reduced to Pt metal, but there is a decrease in binding energy to the extent of charge transfer from hydrogen to the metal ion. There was no significant shift that could be measured in the core level binding energies of Ce(3d) and O(1s). Further, upon hydrogen adsorption, hydroxyl OH^- were not developed in the O(1s) region at ~531.5 eV compared to O(1s) of the O^{2-} ion at 530.3 eV.

3.2. Simulations. *3.2.1. Stability.* Calculation of energies per hydrogen of different structures is compared in the following way: $[E_{slab}(Ce_{15}PtO_{31} + nH) - E_{slab}(Ce_{15}PtO_{31}) - nE(H)]/n$ where E_{slab} is the total energy for the slab calculations, $E(H)$ is the total energy for a single hydrogen atom, and n is the number of H's on the CeO_2/*Pt* surface. These energies are −3.448, −3.465, −2.501, −3.327, −3.455, −3.426, and −3.001 eV per H atom for 1, 2, 3, 4, 5, 6, and 7 H's on CeO_2/*Pt*. This shows that the 2-H case is the most stable and the stability is least for the 3-H case. The minimum stability for the 3-H case can be understood from the bond lengths of H with other atoms and the presence of all dissociated H's with no spillover; these are discussed later. For reference, our estimate of the energy ($[E(H_2) - 2E(H)]/2$) for H_2 is −3.004 eV/atom.

3.2.2. Bond Lengths: Dissociated and Spilled Hydrogens. We have investigated the spillover phenomena from the understanding of bond lengths (H−Pt, H−O, H−Ce), net charges on atoms, and net energies for hydrogen binding on the catalyst surface. Although Pt metal is known to hold one hydrogen per Pt atom, platinum in the ionic state is expected to hold more than one hydrogen because of charge transfer between Pt and hydrogens. The Pt ion can easily hold one or two hydrogen atoms, and as the number of hydrogen atoms increase, the distance of hydrogens from Pt increases, resulting in the interaction of hydrogen with other ions. H−H distances are also an important issue, as the hydrogen present in the dissociated state might determine the number of nascent/active hydrogens generated on the CeO_2/Pt matrix. Also the total number of hydrogen atoms stabilized on the CeO_2/Pt matrix gives an estimate of the amount of hydrogen that can be stored by the Pt-doped ceria matrix and hence of the enhancement with respect to hydrogen storage over Pt metal and pure ceria.

(23) Briggs, D.; Seah, M. P. *Practical Surface Analysis*; John Wiley and Sons: New York, 1983; p 119.

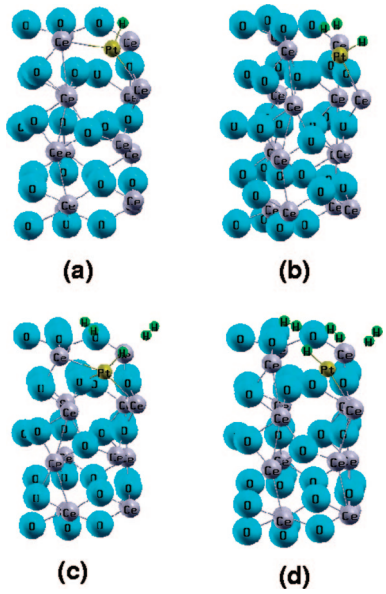

Figure 6. Structures with odd number of hydrogens on *CeO_2/Pt* in a single cell: (a−d) for 1, 3, 5, and 7 hydrogens, respectively.

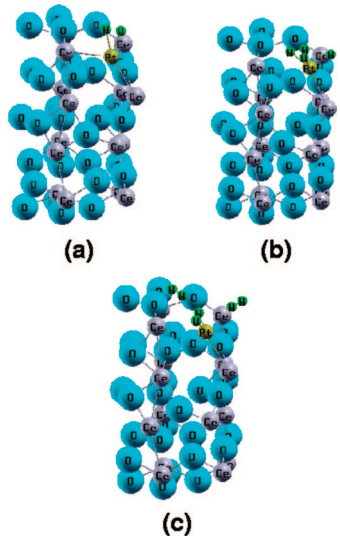

Figure 7. Structures with even number of hydrogens on *CeO_2/Pt* in a single cell: (a−c) 2, 4, 6 hydrogens, respectively.

Considering the minimum H−H bond length about 0.74 Å for hydrogen molecule formation, any H−H bond length greater than 0.74 Å and less than 0.82 Å is taken as bond length for partly dissociated hydrogens or a precursor to partial dissociation. For H−H bond lengths of 0.82 Å and above (as seen for the 3-H case with all dissociated hydrogens), the hydrogens are considered to be in fully dissociated form or a precursor to full dissociation. The H−H distance of 0.82 Å is about 10.8% greater than the molecular H−H distance, and at such a distance, the two hydrogen atoms are expected to be far enough as not to form a molecule anymore but to move toward the dissociated state. Figure 6 and Figure 7 show the structures with odd and even number of hydrogens, respectively. The H−Pt, H−Ce, and H−O minimum distances are taken as 1.59, 2.54, and 2.71 Å, respectively, as seen for the 3-H case (see Figure 8). The H−Pt distances in all other cases are greater than 1.59 Å. Any H that comes closer than the cutoff distance of ions is

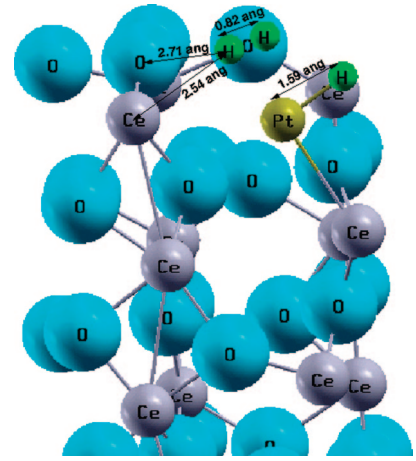

Figure 8. Magnified figure for the 3-H case showing the H−H minimum distance for dissociated H's and minimum H−Pt, H−Ce, and H−O distances.

Table 1. Dissociated and Spillover Hydrogens

no. of hydrogens	type of hydrogens
1	1 (dissociated)
	0 (spillover)
2	2 (dissociated)
	0 (spillover)
3	3 (dissociated)
	0 (spillover)
4	4 (dissociated)
	3 (total spillover):
	[2 (spillover to oxygen, dissociated),
	1 (spillover to oxygen and cerium, dissociated)]
5	1 (dissociated)
	4 (molecule like)
	2 (total spillover):
	[1 (spillover to oxygen, molecule),
	1 (spillover to oxygen and cerium, molecule)]
6	2 (dissociated)
	2 (slightly dissociated)
	2 (molecule like)
	3 (total spillover):
	[3 (spillover to oxygen, 2 dissociated and 1 molecule)]
7	1 (dissociated)
	2 (slightly dissociated)
	4 (molecule like)
	5 (total spillover):
	[2 (spillover to oxygen, molecule),
	2 (spillover to cerium, 1 molecule and 1 dissociated),
	1 (spillover to oxygen and cerium, molecule)]

considered to be spilled over to that particular ion. We find that the maximum number of dissociated hydrogens is 4 and as the number of hydrogens is increased up to 7, the number of dissociated hydrogens decreases and more slightly dissociated and molecular species start forming (see Table 1). There is no spillover of hydrogen atoms up to the 3-H case, and spillover starts from the 4-H case with maximum spillover of 75%, i.e., three out of four H's are spilled over. For the 7-H case, there is spillover only to cerium as well, having a total of 71.4% spilled over hydrogens, i.e., five out of seven H's are spilled over. The maximum spillover involving oxygen is 3. The 4-H case is special, where we have maximum active/dissociated hydrogens.

3.2.3. Charge Densities. The net charge of Pt (see Table 2) is at a maximum for the 4-H case and a minimum for 6-H case. The maximum positive charge on Pt for the 4-H case reflects that maximum charge is transferred out of Pt,

Table 2. Net Hirshfeld Charges on Pt, Average Net Charge on Surface Ce and O Ions on the Pt-Doped Side of the Surface, Total Average Net Charge on the Surface Ions with Respect to Hydrogen-Free Case

no. of hydrogens	Q_{Pt}	Q_{Ce}	Q_O	matrix surface charge
0	0.3637	0.7612	−0.4195	1.0000
1	0.3743	0.7536	−0.4195	1.0043
2	0.3051	0.7444	−0.4165	0.8974
3	0.3958	0.7346	−0.4250	1.0000
4	0.4547	0.7206	−0.4273	1.0604
5	0.3974	0.7361	−0.4239	1.0060
6	0.2936	0.7345	−0.4010	0.8890
7	0.3702	0.7167	−0.4137	0.9544
pure CeO_2		0.7740	−0.4309	

Table 3. Net Charge on Hydrogen

no. of hydrogens	Q_H
1	0.05818
2	0.05694, 0.05847
3	0.03804, 0.05742, 0.06707
4	0.05696, 0.05384, 0.04914, 0.05696
5	0.03613, 0.04555, 0.00128, 0.02110, −0.00807
6	0.00447, 0.02258,0.00079, −0.00442, 0.02281, 0.00447
7	0.03590, 0.00647, 0.04670, 0.01428, −0.00295, −0.00009, 0.05075

hence maximum interaction with surrounding atoms. For surface Ce atoms, the net positive charge is reduced as the number of hydrogen increases up to the 4-H case, again increases for 5 and 6 H's, and is the least for the 7-H case. This means that, initially, the negative charge transfer into Ce is less and increases as the number of hydrogens increase up to the 4-H case, correlating with spillover to Ce. The Ce net charge is the least in the case of 7-H, showing maximum negative charge transfer into surface Ce atoms because of maximum spillover to Ce. The net charge on surface oxygen atoms is at a minimum for the 6-H case and a maximum for the 4-H case. The minimum negative charge on oxygens for the 6-H case is due to maximum flow of charge out of oxygens, as there is spillover to oxygens only. The ratio of the average net surface charges on Pt, Ce, and O for different number of hydrogens with respect to that of the hydrogen-free case shows that the surface charge in the matrix of Pt, Ce, O ions is maximum for the 4-H case and minimum for the 6-H case. From the DFT calculations, Hirshfeld net charge on Pt ion is 0.3637 and the minimum net charge on Pt for the six-hydrogen case is 0.2936. For a decrease of 0.07 charge, a lower binding energy shift of about 0.29 eV is expected. This is close to the observed value of 0.3 eV from the experimental XPS data (see Figure 5). Therefore, Hirshfeld charges on the ions do give direction of charge transfer.

For all the slabs with hydrogen, the average net charges of Ce and O on the hydrogen-free surface of the slab remain unaffected by the number of hydrogens on the other surface of the slab (Pt-doped surface) and are close in value to the surface charges of the slab without hydrogen. The net charges of Ce and O atoms in the bulk layers of the slab also remain unaffected by presence of hydrogens on the surface.

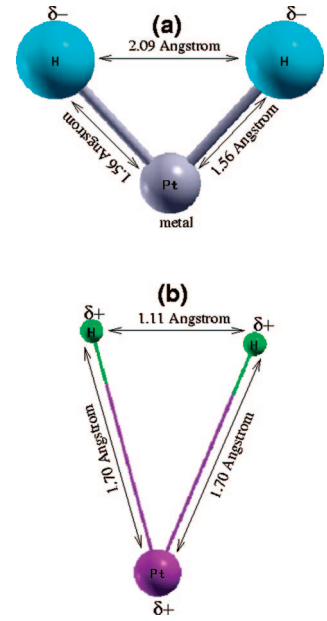

Figure 9. (a, b) Final configurations of Pt^0 (metal) and Pt^{2+}, respectively, with hydrogen molecule interaction.

The average net charges on hydrogens (see Table 3) for 1-, 2-, 3-, and 4-H cases are 0.05818, 0.05771, 0.05418, and 0.05423, respectively, which are close in value, whereas for the other cases, the average net charge reduces. The hydrogen having negative charge for the 5-H case is dissociated and is closest to Pt compared to other hydrogens. For the 6- and 7-H cases, one of the hydrogens having negative charge has a tendency to form $H^{\delta+}-H^{\delta-}$ species with a hydrogen having strong positive net charge, whereas the other hydrogen of the 7-H case having a negative net charge is dissociated and is closest to Pt compared to the other hydrogens.

3.2.4. Pt^0 and Pt^{2+} Interaction with Hydrogen. We have simulated interaction of an isolated platinum atom (Pt^0) with hydrogen. One hydrogen at an initial distance of 1.80 Å from one Pt^0 comes closer to platinum at a distance of 1.57 Å, which is 1% less than the minimum distance of hydrogen from a Pt ion in the ceria matrix. Further, the net charges of platinum and hydrogen are 0.0262 and −0.0259, respectively. Thus, the adsorbed hydrogen atom on Pt^0 is hydridic. A molecule of hydrogen placed with its center at an initial distance of 1.80 Å from an isolated Pt^0, dissociates fully with a large H−H distance of about 2.09 Å and are closely bound to the platinum metal with a hydrogen−platinum distance of 1.56 Å, which is closer than the minimum H−Pt (ion) distance in the ceria matrix (see Figure 9). The net charge on platinum is 0.0197 and the net charge on each of two hydrogens is same, of about −0.0097. Hence a hydrogen molecule placed near Pt^0 forms platinum hydride (PtH_2)-like species, which is rather different from the interaction of hydrogen with platinum ion in the ceria matrix.

Huda and Kleinman[24] have investigated hydrogen adsorption and dissociation on small unsupported platinum clusters (up to 5 Pt atoms), using DFT calculations. Their results for PtH_2 with a H−H separation of 2.09 Å on Pt are exactly same as those obtained from our calculations of isolated Pt^0

(24) Huda, M. N.; Kleinman, L. *Phys. Rev. B* **2006**, *74*, 195407.

and H_2. The Pt−H distance from the above reference is 1.53 Å (close to our obtained value of 1.56 Å). For a single H atom on Pt, the Pt−H distance from the above reference is 1.54 Å (close to our obtained value of 1.57 Å). All the calculations in the above reference have been done with the generalized gradient approximation (GGA) to the exchange-correlation and used spin–orbit coupling, whereas our calculations are done with LDA without spins. There is good agreement between the above paper and our calculations for Pt^0.

To check the interaction of a platinum ion with hydrogen, we placed a hydrogen molecule at an initial distance of 1.80 Å centered at an isolated Pt^{2+} ion. We created the Pt^{2+} ion by making the entire system deficient of two electrons. In the final configuration, the molecule dissociates with a H−H distance of 1.11 Å and H−Pt distance of 1.70 Å, which are similar to the bond lengths of the 2-H case on CeO_2/Pt (H−H distance is 0.92 Å and H−Pt distances are 1.76 and 1.72 Å). Charge density analysis of the final configuration shows protonic hydrogens each having a net charge of 0.2679, and the net charge on Pt is 1.4642. On the other hand, one hydrogen placed near an isolated Pt^{2+} ion at 1.80 Å is unstable and goes off to a large distance of 7.92 Å in the final configuration, but the net charges on Pt (1.2628) and hydrogen (0.7373) remain positive, verifying the repulsive electrostatic interaction. In CeO_2/Pt however, the H−Pt distance is small, about 1.61 Å, indicating the crucial role of ceria matrix.

A Pt atom has been substituted for Ce with an oxygen atom vacancy in ceria. The formal valence of Pt in $Ce_{15}PtO_{31}$ is +2. In our calculations, we cannot constrain the ionicity of Pt directly, but we can simulate a chemical environment like oxygen vacancy, with which a desired ionicity of Pt can be imposed to some extent. In the case of isolated Pt ion and hydrogen calculations, we have tried to investigate the role of the Pt ion only upon removal of two electrons from the system. Similarly, in these calculations, we cannot do simulations of Pt ion and hydrogen directly, but are able to create a system that is electron deficient. Our pseudopotentials are transferable in the sense that they work well for both neutral atoms and ions. Hence, it depends on how we create a system in DFT calculations for the atoms to exist in the neutral state or in ionic state.

4. Conclusions

In conclusion, we have theoretically stabilized up to 7 hydrogen atoms (per cell) on CeO_2/Pt matrix compared to 1 H/Pt for pure platinum surface and shown that hydrogen atoms are found in two chemical states dissociated and molecular. The maximum number of fully dissociated hydrogens is found to be four, as seen in the 4-H case, whereas the number of fully dissociated hydrogens reduce as the concentration of hydrogen is increased beyond 4 H's. Up to 3 H's, there is no spillover, whereas spillover is maximum for the 4-H case. The maximum distance from Pt to which hydrogen is spread on the matrix is for the 5-H case, about 4.14 Å; the farthest hydrogen is in the molecular form with another hydrogen and is spilled to oxygen and Ce. The Pt−Pt distance is about 7.65 Å and the H−H distance for the two distant hydrogens around neighboring Pt ions is about 3.40 Å, so there is no influence of a neighboring Pt ion and no bond formation between hydrogens around neighboring Pt ions. The Pt ion in CeO_2 certainly plays a dominating role in the dissociation of molecular hydrogen placed near it to protonic species, which is clear in the case of 2-H CeO_2/Pt and for the isolated Pt^{2+} ion and hydrogen molecule interaction. The maximum number of protons formed on the CeO_2/Pt surface is 5, as found up to the 7-H case; the large number of dissociated protons (positively charged hydrogens) are clearly the active species produced on the catalyst surface (confirmed by NMR study for Pt ion in the CeO_2 system and simulation of isolated Pt ion and hydrogen interaction), which are important for any reduction reaction. The Pt metal (Pt^0) interaction with hydrogen results in hydrogens having negative net charge (hydridic) that are more closely bound to Pt^0 than with Pt ion, and these species of hydrogens will not be active in any reduction reaction. There is also no formation of OH^- ions, as the O−H distance is much larger than the bond length of hydroxyl ion (which is about 0.958 Å) and no water is formed on the catalyst because of interaction with hydrogen. Thus, CeO_2/Pt helps in production of active hydrogen and the spillover of hydrogen, thus increasing the hydrogen storage in the matrix with the H/Pt ratio much greater than one.

Acknowledgment. We thank the central computing facility at JNCASR and CDAC (Bangalore) for use of computational resources. G.D. thanks UGC and CCMS (JNCASR) for research fellowships. We thank DST for financial support for experimental work. We especially thank Sankeerth Hebbar and Uday Prabhu of the NMR Research Centre, IISc, Bangalore, for their help in NMR data collection.

CM071330M